
01 Aug 2007

Crystal and Electronic Structures of the Complex Hydride $\text{Li}_4\text{BN}_3\text{H}_{10}$

Jinbo Yang

X. J. Wang

Qingsheng Cai

William B. Yelon

Missouri University of Science and Technology, yelonw@mst.edu

et. al. For a complete list of authors, see https://scholarsmine.mst.edu/phys_facwork/337

Follow this and additional works at: https://scholarsmine.mst.edu/phys_facwork

 Part of the [Chemistry Commons](#)

Recommended Citation

J. Yang et al., "Crystal and Electronic Structures of the Complex Hydride $\text{Li}_4\text{BN}_3\text{H}_{10}$," *Journal of Applied Physics*, American Institute of Physics (AIP), Aug 2007.

The definitive version is available at <https://doi.org/10.1063/1.2767253>

This Article - Journal is brought to you for free and open access by Scholars' Mine. It has been accepted for inclusion in Physics Faculty Research & Creative Works by an authorized administrator of Scholars' Mine. This work is protected by U. S. Copyright Law. Unauthorized use including reproduction for redistribution requires the permission of the copyright holder. For more information, please contact scholarsmine@mst.edu.

Crystal and electronic structures of the complex hydride $\text{Li}_4\text{BN}_3\text{H}_{10}$

J. B. Yang^{a)} and X. J. Wang*Graduate Center for Materials Research, University of Missouri-Rolla, Rolla, Missouri 65409
and Department of Physics, University of Missouri-Rolla, Rolla, Missouri 65409*

Q. Cai

Department of Physics, University of Missouri-Columbia, Columbia, Missouri 65211

W. B. Yelon and W. J. James

*Graduate Center for Materials Research, University of Missouri-Rolla, Rolla, Missouri 65409
and Department of Chemistry, University of Missouri-Rolla, Rolla, Missouri 65409*

(Received 20 March 2007; accepted 20 June 2007; published online 7 August 2007)

The crystal structure of $\text{Li}_4\text{BN}_3\text{H}_{10}$ was investigated using powder neutron diffraction with high sensitivity. The compound crystallizes in the cubic space group $I2_13$ with lattice parameters $a = 10.645\ 19(52)$ Å with an ordered arrangement of $[\text{NH}_2]^{-1}$ and $[\text{BH}_4]^{-1}$ anions in a molar ratio of 3:1. The bond lengths between the nearest nitrogen and hydrogen atoms are 1.04(4) and 1.14(4) Å. The bond angle between H(1)–N–H(2) is about $126(6)^\circ$, while those between H(3)–B–H(3) and H(3)–B–H(4) are about $109(6)^\circ$ – $110(7)^\circ$. There are three different Li sites surrounded by $[\text{NH}_2]^{-1}$ and $[\text{BH}_4]^{-1}$ anions in distorted tetrahedral configurations. The Li(3)–B and Li(3)–N bond distances are about 1.72(3) and 2.32(2) Å, respectively, while the Li(1)–N and Li(2)–N distances are both around 2.09 Å. The strong bonding of Li(3) to the $[\text{BH}_4]^{-1}$ and the weaker Li(3)– $[\text{NH}_2]^{-1}$ bond are evidenced by the presence of the LiBH_4 moiety in a projection of the crystal structure onto the a - b plane. First-principle calculations have been performed based on the structural data. Analyses of the density of states and charge density indicate that H(1) and H(2) strongly interact with N, and H(3) and H(4) interact with B to form $[\text{NH}_2]^{-1}$ and $[\text{BH}_4]^{-1}$, respectively. It is confirmed that Li(1) and Li(2) are strongly bonded to N and Li(3) is strongly bonded to B. These results are significantly different from some of the previous studies. © 2007 American Institute of Physics.

[DOI: [10.1063/1.2767253](https://doi.org/10.1063/1.2767253)]

I. INTRODUCTION

The challenge of developing reversible hydrogen storage systems for vehicular applications remains unsolved. A variety of compounds with sufficient capacity have been identified, but these are beset by a variety of problems, such as high decomposition temperature and poor reversibility. Some of these problems have been partially solved through the addition of catalysts, but these additions decrease the overall hydrogen density and the long term reversibility of the systems remains doubtful. Much of the ongoing research has focused on alanates $M\text{AlH}_4$ and tetrahydroborides $M\text{BH}_4$, where M is an alkali metal.^{1–22} Recently, compounds formed from stoichiometric mixtures of LiNH_2 and LiBH_4 in ratios of 1:1, 2:1, and 3:1 have been shown to form compounds that contain large quantities of hydrogen as high as 11.9 wt % in the case of $\text{Li}_4\text{BN}_3\text{H}_{10}$, and therefore may be useful.^{23–28} The crystal structure of $\text{Li}_4\text{BN}_3\text{H}_{10}$ was determined by Filinchuk *et al.* using single crystal synchrotron x-ray diffraction.²⁶ The structure was reinvestigated by Noritake *et al.*, using synchrotron x-ray powder diffraction,²⁷ and by Chater *et al.* using synchrotron x-ray and neutron powder diffraction.²⁸ However, the refined structures were not consistent between these three studies. For example, Noritake *et al.*²⁷ used two nitrogen sites and two lithium sites to refine the structure;

whereas Filinchuk *et al.*²⁶ and Chater *et al.*²⁸ used three Li sites and one N site in this structure. Furthermore, the ND study of Chater *et al.*²⁸ appeared to use significantly different crystallographic parameters as compared to the synchrotron x-ray studies.^{26,27} Our examination of the models by Filinchuk *et al.* and Chater *et al.* shows them to be equivalent. To date, definitive structural parameters for $\text{Li}_4\text{BN}_3\text{H}_{10}$ have not been published. Such information is important to an understanding of the basic hydrogen storage properties of this compound. The main issue in the x-ray structural analysis for compounds such as the light metal hydride $\text{Li}_4\text{BN}_3\text{H}_{10}$, with low atomic numbers, is their poor scattering cross sections for x rays. The intensity of coherently diffracted x rays is proportional to the square of the atomic number, and accurate observation of hydrogen is always problematic. In contrast, neutron scattering from the hydrogen proton (or often, the deuteron) gives a reliable measurement of the hydrogen (deuteron) location and occupation. Hydrogen possesses a large incoherent cross section (related to processes in which the neutron and hydrogen atom spins flip during the interaction). These processes lead to a large, featureless background in the diffraction pattern, reducing the statistical accuracy of the final result. Thus, deuterium, with a much smaller incoherent scattering cross section, is often employed. The replacement of the hydrogen with deuterium improves the diffraction pattern but does not necessarily provide the exact hydrogen locations.²⁹ Kinetic properties are also affected by

^{a)} Author to whom correspondence should be addressed; electronic mail: jinbo@umr.edu

H–D replacement. Knowledge of the structural properties of $\text{Li}_4\text{BN}_3\text{H}_{10}$, especially the accurate location of the hydrogen atoms, is critical to an understanding of and improvement in the hydrogen absorption and desorption capacity of the system. In the present paper, we have used neutron powder diffraction to determine the crystal structure for $\text{Li}_4\text{BN}_3\text{H}_{10}$. First-principle calculations based on the structural data were performed to study the fundamental properties of this compound.

II. METHODS

$\text{Li}_4\text{BN}_3\text{H}_{10}$ was prepared by reacting a 5 gm mixture of LiNH_2 and LiBH_4 powders (purchased from Sigma-Aldrich) in a 3:1 molar ratio by high energy ball milling in a stainless steel vial with a ball to sample mass ratio of 20:1. The milling time was 6 h. Part of the as-prepared powders was annealed at 170 °C for 2 days. Using a similar procedure, $\text{Li}_3\text{BN}_2\text{H}_8$ ($\text{LiNH}_2:\text{LiBH}_4=2:1$) and Li_2BNH_6 ($\text{LiNH}_2:\text{LiBH}_4=1:1$) were prepared. For the diffraction measurements, the Li–B–N–H powders were put into 3 mm diameter thin-wall vanadium containers and sealed in a glovebox under an argon atmosphere to avoid reaction with moisture. The powder neutron diffraction (ND) experiments were performed on the position sensitive detector diffractometer at the University of Missouri Research Reactor using neutrons of wavelength $\lambda=1.4875$ Å. The data for as-prepared and annealed samples were collected over 24 h at 290 K between 2θ angles of 5° and 105° on approximately 1.0 g of fine powders. The refinement of the neutron diffraction data was carried out using the FULLPROF program³⁰ which permits multiple phase refinement.

The electronic structure was calculated using the WIEN2K code.³¹ The full potential linearized augmented plane wave method was employed using the density function theory within the generalized-gradient approximation (GGA). The radii of the atomic spheres are 1.61, 1.46, 1.27, and 0.69 a.u. for Li, B, N, and H, respectively. The upper limit of the angular momentum, $l_{\text{max}}=10$, is adopted in the spherical-harmonic expansion. A cutoff energy of 457 eV and a 512 k -point grid in the irreducible Brillouin zone were used in the calculations. The convergence is obtained with 10^{-6} eV of the total energy.

III. RESULTS AND DISCUSSION

Figure 1 shows the room temperature neutron powder diffraction patterns of $\text{Li}_4\text{BN}_3\text{H}_{10}$ before and after annealing. The background is mainly due to the incoherent scattering of hydrogen atoms. Even though the incoherent scattering of hydrogen and absorption of ^{10}B are strong, the diffraction intensities are high due to the special design of our ND system, which uses a very small sample size, minimizing multiple scattering into the incoherent channel. The peaks of the annealed sample are much higher and sharper than the as-prepared sample, especially in the high angle region, due to the higher degree of crystallinity. This significantly improves the quality of the diffraction pattern, which enables an accurate determination of the atomic positions of H and B in this compound. The pattern can be indexed in a cubic cell with

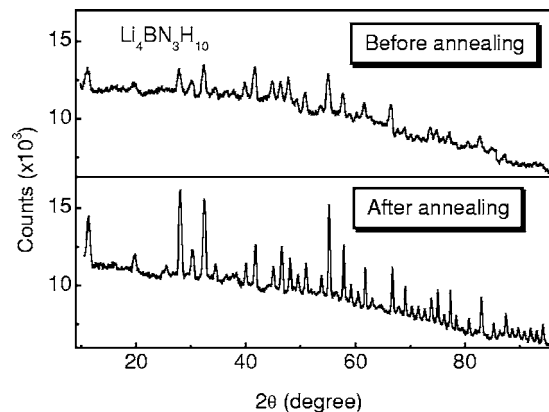


FIG. 1. Neutron diffraction patterns of $\text{Li}_4\text{BN}_3\text{H}_{10}$ at room temperature.

space group $I2_13$ with $a=10.64519(52)$ Å. The unit cell has eight formula units. We chose to refine the atomic positions of each atom using two different models, that of Filinchuk *et al.* (I) (Ref. 26) and of Noritake *et al.* (II).²⁷ The atomic positions for model (I) are Li(1)(12b)($x,0,1/4$), Li(2)(12b)($x,0,1/4$), Li(3)(8a)(x,x,x), and N(24c)(x,y,z), respectively. The atomic positions for model (II) are N(1)(12b)($x,y,1/4$), N(2)(12b)($x,y,1/4$), Li(1)(24c)(x,y,z), and Li(2)(24c)(x,y,z). In both models, hydrogen atoms were assumed at four positions H(1)(24c)(x,y,z), H(2)(24c)(x,y,z), H(3)(24c)(x,y,z), and H(4)(8a)(x,x,x), and boron at B(8)(24a)(x,x,x). The thermal parameters for each atom type were constrained to be equal.

Figure 2(a) shows the refined patterns with model I, which gives a good fit to the data. Figure 2(b) plots the calculated pattern based on model I, using the parameters of Noritake *et al.*²⁷ It clearly fails to reproduce the data. In

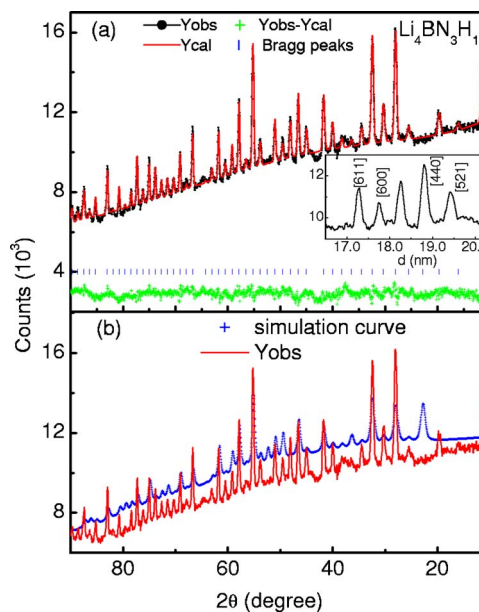


FIG. 2. (Color online) (a) Refined neutron diffraction pattern with model I. In the patterns, the bottom curves ($Y_{\text{obs}}-Y_{\text{cal}}$) are the difference between experimental data and refinement data. The vertical bars indicate Bragg peak positions. The inset indicates the indexed peaks, showing increasing d spacing to allow sample comparison (the [440] peak appears at about 46.47° (2θ)), with data in Ref. 28. (b) The calculated pattern of $\text{Li}_4\text{BN}_3\text{H}_{10}$ with model II (symbol +) and the experimental data (solid line).

TABLE I. Refined parameters of $\text{Li}_4\text{BN}_3\text{H}_{10}$ at room temperature. Space group is $I2_13$ with $a = 10.664\ 519(52)$ Å. x , y , z are the fractional position coordinates; and n is the occupation number. d is the nearest neighbor distance. χ^2 is 2.90%. The values in the brackets are data from Ref. 26.

Wyckoff site		x	y	z	n
Li(1)	12b	0.286 80(246) {0.287 1}	0	0.25	0.5
Li(2)	12b	0.521 99(310) {0.523 7}	0	0.25	0.5
Li(3)	8a	0.517 17(243) {0.483 30}	x	x	0.3333
N	24c	0.112 08 (43) {0.115 36}	0.360 22 (51) {0.359 31}	0.403 94 (59) {0.405 25}	1.0
B	8a	0.110 14 (142) {0.113 60}	x	x	0.3333
H(1)	24c	0.167 93 (376) {0.175 1}	0.279 69(289) {0.3100}	0.398 10 (393) {0.3969}	1.0
H(2)	24c	0.123 62 (294) {0.114 5}	0.449 13 (372) {0.4051}	0.345 13(408) {0.3391}	1.0
H(3)	24c	0.002 23(173) {0.012 3}	0.122 94(352) {0.1194}	0.138 17(503) {0.1460}	1.0
H(4)	8a	0.179 38(467) {0.172 1}	x	x	0.3333

		$d(\text{Å})$				
	Li-B	Li-N	B-H		H-N	H-H
Li(1)	2.67 {2.65}	2.085 {2.1147}	B-H(3) 1.19 {1.137}	H(1)-N 1.04 {0.83}		1.94
Li(2)	>4.0	2.093 {2.1166}	B-H(4) 1.27 {1.08}	H(2)-N 1.14 {0.859}		2.02
Li(3)	1.73 {2.41}	2.320 {2.0689}				2.30

Table I, we list the refined atomic positions and nearest neighbor distances for model I. For comparison, we also list the atomic positions of Filinchuk *et al.*²⁶ Although the model by Filinchuk *et al.* is successful, the positions we obtained for the hydrogen and Li(3) atoms are significantly different from their values, dramatically changing the bond distances and angles between N-H and Li-B. The nearest neighbor distances of N-H(1) and N-H(2) are 1.04(4) and 1.14(4) Å, respectively, which are much longer than the reported values ($d_{\text{N-H}}=0.83$ and 0.86 Å).²⁶ The H-N-H bond angle is about $126(6)^\circ$. These values are close to those of LiNH_2 and LiND_2 (Refs. 32–34) ($d_{\text{N-D}}=1.01$ Å). The bond distances are 2.085, 2.093, and 2.32 Å for Li(1)-N, Li(2)-N, and Li(3)-N, respectively. The Li-B bond distances are 2.67 and 1.73 Å for Li(1)-B and Li(3)-B, respectively. The Li(3)-B distance is much shorter than the shortest Li-B distance (2.475 Å) in LiBH_4 .⁴ At the same time, the B-H bond lengths are about 1.19–1.27 Å: longer than the B-H bond distance, 1.03 Å, in LiBH_4 ,¹² and the N-H bonds are longer than those of LiNH_2 as well,^{32,33} suggesting that the Li(3)-B bond has strengthened at the expense of the B-H bonds. The longer bond distances indicate a decrease in the B-H and N-H bonding energy, which could enhance the hydrogen release under practical conditions. Pinkerton *et al.*²³ have shown that $\text{Li}_4\text{BN}_3\text{H}_{10}$ can release >10 wt % hydrogen above 250 °C with ammonia present only in trace amounts.

Chater *et al.*²⁸ and Filinchuk *et al.*²⁶ employed the same model as we used. While the differences between our refinement and that of Filinchuk *et al.* might be attributed to their

use of x rays, Chater *et al.* used both neutrons and x rays and therefore better agreement with our results would be expected. Comparison of our diffraction data with that of Chater *et al.*²⁸ does reveal some significant differences. For example (see inset), the peak intensity ratios of the [521]/[440] are about 1.0/2.0 for our data and about 1.0/1.0 for theirs, and the ratios of the peaks [600] are [611] about 2:1 and 3:1 for our data and theirs, respectively. These differences may result from compositional differences between our sample and theirs due to different preparation processes. In fact, the neutron data from Chater *et al.* more closely resemble our results for a 2:1 LiNH_2 - LiBH_4 sample, see Fig. 3. We were unable to refine the 2:1 samples using the structural parameters of Filinchuk *et al.*²⁶ and Chater *et al.*²⁸

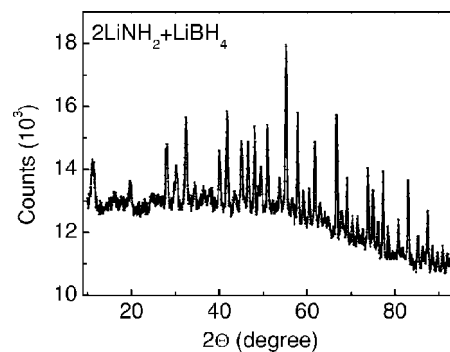


FIG. 3. Neutron diffraction pattern of $\text{LiNH}_2/\text{LiBH}_4=2:1$ sample at room temperature.

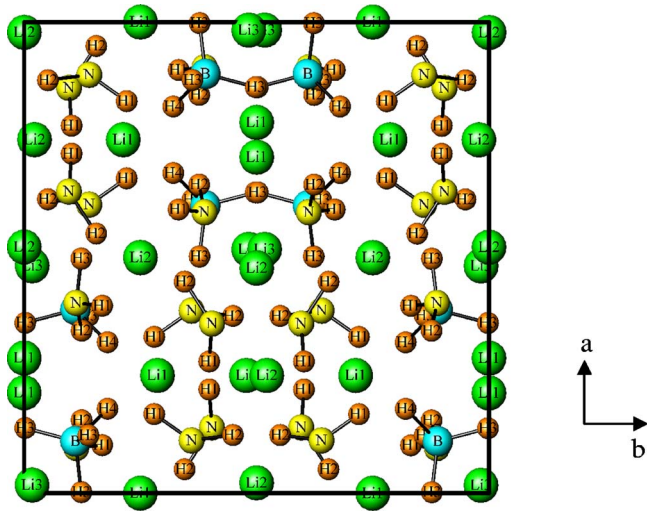


FIG. 4. (Color online) Projection of $\text{Li}_4\text{BN}_3\text{H}_{10}$ crystal structure on the a - b plane.

Furthermore, our ND pattern appears to be that of a dominant 3:1 phase with some LiBH_4 . Indeed, studies, in progress of varying stoichiometries $\pm 3/1$ ratios of $\text{LiN}_2/\text{LiBH}_4$, strongly suggest that this system may be a solid solution system as also pointed out by Chater *et al.*²⁸ If so this could well account for the structural differences observed by all parties. In addition, our data appear sharper in the high q region and the data by Chater *et al.* do not include the lowest order reflections. The refined crystal structure of $\text{Li}_4\text{BN}_3\text{H}_{10}$ is shown in Fig. 4. It consists of an ordered arrangement of $[\text{NH}_2]^{-1}$ and $[\text{BH}_4]^{-1}$ anions with a ratio of 3:1. Nitrogen and two hydrogen atoms, H(1) and H(2), form the $[\text{NH}_2]^{-1}$ anion, while boron and three H(3) and one H(4) atoms form the BH_4^- anions. The $[\text{NH}_2]^{-1}$ and $[\text{BH}_4]^{-1}$ anions in $\text{Li}_4\text{BN}_3\text{H}_{10}$ are similar in configuration to those in the LiNH_2 and LiBH_4 compounds, respectively, while the Li atoms, especially the environment of the Li(3) atom indicates a strong Li(3)– BH_4 bond and a weaker Li(3)– NH_4 bond. Li(1) has two B and two N atoms as its nearest neighbor, Li(2) has four N neighbors, and Li(3) has one B and three distant N atom neighbors.

The calculated density of states (DOS) based on the refined structure of $\text{Li}_4\text{BN}_3\text{H}_{10}$ is shown in Fig. 5. The total DOS shows an energy gap of 2.7 eV between the valence and conduction bands, which indicates a nonmetallic nature. The band gap is smaller than those of LiNH_2 and LiBH_4 . The covalent interaction between the 2s orbital of the nitrogen atom and the 1s electrons of the hydrogen atom dominates the bottom of the valence band interaction. The contribution of the Li orbitals to the DOS is extremely small. The interactions between N-2p and H-1s, B-2s and H-1s electrons contribute to the DOS in the middle energy region, and the N-2p and B-2p orbitals are dominant near the Fermi energy. The N-s, p and H-s states of H(1) and H(2) are energetically degenerate in the entire energy range indicating the formation of the $[\text{NH}_2]^{-1}$ anions, while B-s, p and H-s states of H(3) and H(4) atoms overlap to form the $[\text{BH}_4]^{-1}$ anions. The states of Li(3) atoms strongly overlap with the B states indicating a strong interaction between Li(3) and

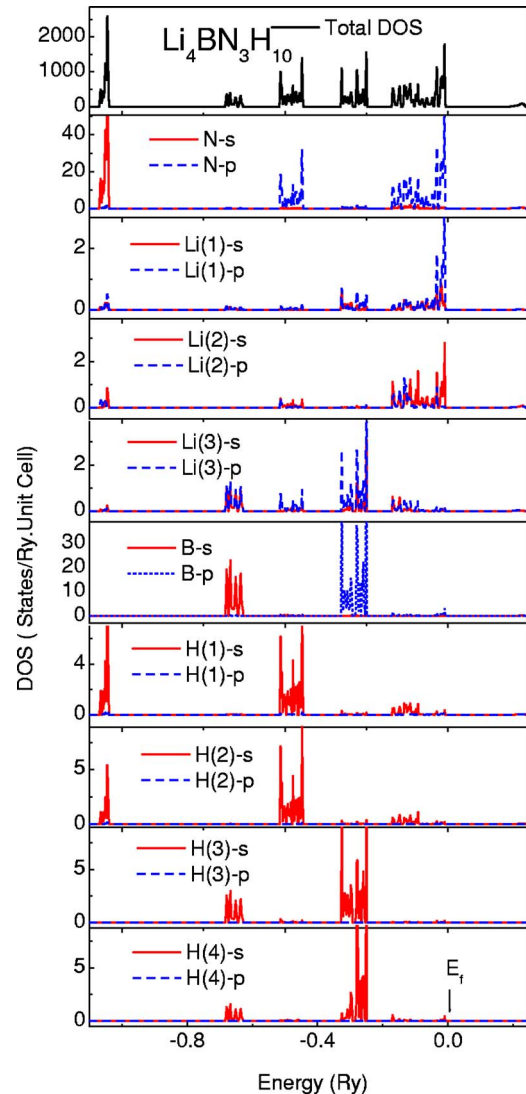


FIG. 5. (Color online) The total and partial DOS of $\text{Li}_4\text{BN}_3\text{H}_{10}$.

$[\text{BH}_4]^{-1}$, while the smaller overlap between Li(3) and N states shows a weaker Li(3)– $[\text{NH}_2]^{-1}$ interaction.

Figure 6 is the calculated valence charge density contour plot of $\text{Li}_4\text{BN}_3\text{H}_{10}$. The $[\text{NH}_2]^{-1}$ and $[\text{BH}_4]^{-1}$ units take the form of well-separated, molecular species distributed over the Li atoms with a rather low charge density between Li^+ and $[\text{NH}_2]^{-1}$ and between Li^+ and $[\text{BH}_4]^{-1}$ as well. The covalent bond nature is dominant within the $[\text{NH}_2]^{-1}$ and

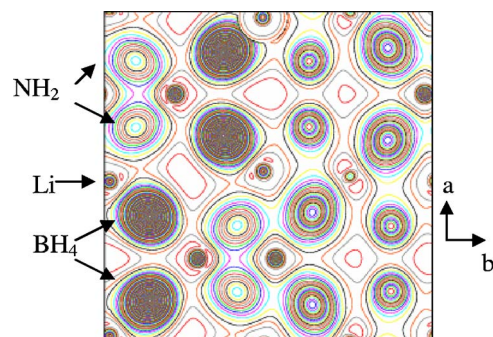


FIG. 6. (Color online) The contours of valence electron density of $\text{Li}_4\text{BN}_3\text{H}_{10}$ in the a - b plane. The contour spacing is $0.01 e/\text{\AA}^3$.

$[\text{BH}_4]^{-1}$ units as can be seen from the charge distribution. The charge densities of the $[\text{NH}_2]^{-1}$ and $[\text{BH}_4]^{-1}$ units show distortion along the direction of their nearest neighbor Li atoms due to the Li^+ -anion interactions.

IV. SUMMARY

In summary, the crystal and electronic structures of $\text{Li}_4\text{BN}_3\text{H}_{10}$ have been investigated using neutron powder diffraction and first-principles calculations. It is found that some atomic positions are significantly different from previous studies. We believe these results more accurately reflect the structure of the stoichiometric 3:1 mixture, while the previous results may be affected by disordered BH_4 substitution of NH_2 anions in samples with a smaller NH_2/BH_4 ratio. The N–H bond lengths are about 1.0 and 1.14 Å for N–H(1) and N–H(2), respectively. The bond angle between H–N–H is 126.0°. H(1) and H(2) strongly interact with N, and H(3) and H(4) interact with B to form $[\text{NH}_2]^{-1}$ and $[\text{BH}_4]^{-1}$, respectively. It is found that Li(1) and Li(2) are strongly bonded to N and Li(3) is strongly bonded to B. $\text{Li}(3)^+ - [\text{NH}_2]^{-1}$ and $\text{Li}(3)^+ - [\text{BH}_4]^{-1}$ interactions are present in the compounds. The electronic structure calculations show that $\text{Li}_4\text{BN}_3\text{H}_{10}$ has strong ionic character. The $[\text{NH}_2]^{-1}$ and $[\text{BH}_4]^{-1}$ anions have strong covalent bonds and their valence charge distributions stretch along the directions of the nearest Li neighbors.

ACKNOWLEDGMENTS

The support by DOE under DOE-BES Contract No. DE-FG02-05ER46245 is acknowledged.

- ¹B. Bogdanovic and M. Schwickardi, *J. Alloys Compd.* **253–254**, 1 (1997).
- ²K. J. Gross, G. J. Thomas, and C. M. Jensen, *J. Alloys Compd.* **330–332**, 683 (2002) and references therein.
- ³C. M. Jensen, R. Zidan, N. Mariels, A. Hee, and C. Hagen, *Int. J. Hydrogen Energy* **24**, 461 (1999).
- ⁴A. Züttel, P. Wenger, S. Rentsch, P. Sudan, Ph. Mauron, and Ch. Emmenegger, *J. Power Sources* **118**, 1 (2003).
- ⁵E. H. Majzoub and K. J. Gross, *J. Alloys Compd.* **356–357**, 363 (2003).
- ⁶A. Zaluska, L. Zaluski, and J. O. Strom-Olsen, *J. Alloys Compd.* **307**, 157 (2000).
- ⁷M. Fichtner, O. Fuhr, and O. Kircher, *J. Alloys Compd.* **356–357**, 418 (2003).
- ⁸R. Genma, H. H. Uchida, N. Okada, and Y. Nishi, *J. Alloys Compd.*

- 356–357**, 358 (2003).
- ⁹H. Morioka, K. Kazizaki, S. Chung, and A. Yamada, *J. Alloys Compd.* **353**, 310 (2003).
- ¹⁰C. M. Jensen, R. Zidan, N. Mariels, A. Hee, and C. Hagen, *Int. J. Hydrogen Energy* **24**, 461 (1999).
- ¹¹A. Züttel, S. Rentsch, P. Fischer, P. Wenger, P. Sudan, Ph. Mauron, and Ch. Emmenegger, *J. Alloys Compd.* **356–357**, 515 (2003).
- ¹²R. A. Zidan, S. Takara, A. G. Hee, and C. M. Jensen, *J. Alloys Compd.* **285**, 119 (1999).
- ¹³C. M. Jensen and K. J. Gross, *Appl. Phys. A: Mater. Sci. Process.* **72**, 213 (2001).
- ¹⁴G. Sandrock, K. Gross, G. Thomas, C. Jensen, D. Meeker, and S. Takara, *J. Alloys Compd.* **330–332**, 696 (2002).
- ¹⁵G. J. Thomas, K. J. Gross, N. Y. C. Yang, and C. Jensen, *J. Alloys Compd.* **330–332**, 702 (2002).
- ¹⁶B. Bogdanovic, R. A. Brand, A. Marjanovic, M. Schwickardi, and J. Tolle, *J. Alloys Compd.* **302**, 36 (2000).
- ¹⁷A. Zaluska, L. Zaluski, and J. Strom-Olsen, *J. Alloys Compd.* **298**, 125 (2000).
- ¹⁸L. Zaluski, A. Zaluska, and J. Strom-Olsen, *J. Alloys Compd.* **290**, 71 (1999).
- ¹⁹H. W. Brinks, C. M. Jensen, S. S. Srinivasan, B. C. Hauback, D. Blanchard, and K. Murphy, *J. Alloys Compd.* **376**, 215 (2004).
- ²⁰M. Fichtner, O. Fuhr, O. Kircher, and J. Rothe, *Nanotechnology* **14**, 778 (2003).
- ²¹B. Bogdanovic, M. Felderhoff, S. Kaskel, A. Pommerin, K. Schlichte, and F. Schuth, *Adv. Mater. (Weinheim, Ger.)* **15**, 1012 (2003).
- ²²K. J. Gross, E. H. Majzoub, and S. W. Spangler, *J. Alloys Compd.* **356–357**, 423 (2003).
- ²³F. E. Pinkerton, G. P. Meisner, M. S. Meyer, M. P. Balogh, and M. D. Kundral, *J. Phys. Chem. B* **109**, 6 (2005).
- ²⁴G. P. Meisner, M. L. Scullin, M. P. Balogh, F. E. Pinkerton, and M. S. Meyer, *J. Phys. Chem. B* **110**, 4186 (2006).
- ²⁵M. Aoki, K. Miwa, T. Noritake, G. Kitahara, Y. Nakamori, S. Orimo, and S. Towata, *Appl. Phys. A: Mater. Sci. Process.* **A80**, 1409 (2005).
- ²⁶Y. E. Filinchuk, K. Yvon, G. P. Meisner, F. E. Pinkerton, and M. P. Balogh, *Inorg. Chem.* **45**, 1433 (2005).
- ²⁷T. Noritake, M. Aoki, S. Towata, A. Ninomiya, Y. Nakamori, and S. Orimo, *Appl. Phys. A: Mater. Sci. Process.* **A83**, 277 (2006).
- ²⁸P. A. Chater, W. I. F. David, S. R. Johnson, P. P. Edwards, and P. A. Anderson, *Chem. Commun. (Cambridge)* **2006**, 2439.
- ²⁹G. E. Bacon and D. H. Titterton, *Zeitschrift fuer Kristallographie, Kristallgeometrie, Kristallphysik Kristallchemie* **141**, 330 (1975).
- ³⁰J. Rodriguez-Carvajal, 1998 Program: FULLPROF, Version 3.d. Available at: <http://www.ill.fr/dif/Soft/fp/php/downloads.html>
- ³¹P. Blaha, K. Schwarz, P. Sorantin, and S. B. Trickey, *Comput. Phys. Commun.* **59**, 399 (1990).
- ³²J. B. Yang, X. D. Zhou, Q. Cai, W. J. James, and W. B. Yelon, *Appl. Phys. Lett.* **88**, 041914 (2006).
- ³³D. B. Grotjahn, P. M. Sheridan, I. Al Jihad, and L. M. Ziurys, *J. Am. Chem. Soc.* **123**, 5489 (2001).
- ³⁴M. Nagib and H. Jacobs, *Atomkernenergie* **21**, 275 (1973).